Environmental Biology of Fishes Vol. 11, No. 4, pp. 277–299, 1984

Early development of the rainbow darter, *Etheostoma caeruleum*, according to the theory of saltatory ontogeny

Michael D. Paine & Eugene K. Balon
Department of Zoology, University of Guelph, Guelph, Ontario N1G 2W1, Canada

Keywords: Percidae, Etheostomatini, Ecomorphology, Embryology, Ecology, Early life history, Heterochrony

Synopsis

The early development of rainbow darter, *Etheostoma caeruleum*, was examined from an ecological perspective. Steps and thresholds of ontogeny to completion of body squammation are defined, and related to environmental factors. Rainbow darter eggs are about 2 mm diameter, considerably larger than those of related logperch (*Percina caprodes*). The embryonic vitelline respiratory plexus is much more extensive. The pelagic interval characteristic of logperch and ancestral percids is eliminated and onset of exogenous feeding is delayed. The larger larvae of the rainbow darter can begin feeding directly on aquatic insects, and complete their life cycle in streams. Therefore, shifts in the timing of important thresholds (e.g. exogenous feeding) are ecologically important. Furthermore, early maturation and/or delayed bone and scale formation may be responsible for reductions in the lateralis system and scalation in this and other darter species.

1. Introduction

The ecological classification of fishes into reproductive guilds (Balon 1975a) rests on the premise that early ontogenies and reproductive styles are correlated, and important ecologically. The hierarchical arrangement of guilds reflects a presumed evolutionary trend from small, unprotected, pelagic young with a prolonged larval period to large, protected, demersal young without a larval period (Balon 1984b). The theory of saltatory ontogeny postulates that development proceeds as a sequence of intervals of relative stasis (steps), separated by rapid switches to new form and function (thresholds) (Balon 1979, 1981a, 1984a). In addition to their epigenetic significance, thresholds are important ecologically when they mark changes in the organism to environment relationship. Shifts in the timing of thresholds (heterochrony) may be responsible for life history patterns and the evolutionary trends reflected in the arrangement of guilds (Balon 1981b, 1983).

This paper continues an examination of the ecological and evolutionary significance of reproductive styles and ontogenies of darters (Percidae: Etheostomatini). Previously, we (Paine & Balon 1984) described the early development of northern logperch (*Percina caprodes semifasciata*), relating it to environmental factors. The apparent restriction of most *Percina* species to ancestral percid habitats (lakes, rivers) was attributed to retention of ancestral developmental patterns, particularly the presence of a pelagic interval. In this study we describe in detail the ecomorphological development of the rainbow darter (*Etheostoma caeruleum*), one of three species briefly examined in an earlier preliminary work (Paine 1984). Steps and threshold are defined, and correlated with environ-

mental requirements. The role of heterochrony in producing the river/stream differences between *Percina* and *Etheostoma* (Paine 1984) is considered, through comparison of rainbow darter and logperch ontogenies.

2. Materials and methods

Adult rainbow darters were captured in Swan Creek, a tributary of the Grand River about 15 km north of Guelph. Fish were transported live to the University of Guelph on 29 April (group 1), 30 April (group 2), 3 May (group 3), 5 May (group 4), and 21 May (group 5), 1981. Each parental group consisted of 7 to 15 fish, with females predominating. Ova were stripped into plastic dishes and fertilized using testes mashed in fish saline (prepared according to Ginsburg 1963). The dishes of eggs were incubated at 19.8–20.2° C in the system described earlier (Paine & Balon 1984). A 15 light: 9 dark hours photoperiod was maintained during incubation. Larvae were fed brine shrimp nauplii, finely ground prepared trout and tropical fish food, and frozen zooplankton.

Procedures followed Paine & Balon (1984), which may be checked for details. Sampling was continuous, involving observation and photographs of the same group of individuals, for the first hour after activation (as defined in Balon 1981a). The sampling declined in frequency with increasing age. Group 1 was used for age 0 to 1 days, group 2 for ages 0 to 4 days and 25 days and older, group 3 for age 2 to 25 days, group 4 for repeating earlier samples and for age 25 days and older, and group 5 for repeating earlier samples. Differences among groups were largely restricted to older specimens and are noted in the Results section.

Drawings of live specimens were made using a C&D projection microscope (Scientific Instruments, Hemel Hempstead, England); photomicrographs were taken through C&D and binocular dissection microscopes using ocular attachments and Minolta RS-T cameras. Before drawings or photographs were made, cardiac pulse was taken. After drawings were completed, specimens were preserved in $CaCO_3$ buffered 10% formalin. Preserved embryos were later stained with alcian blue for cartilage mucopolysaccharide, cleared with trypsin, then stained with alizarin red S for calcium phosphate (Taylor 1967, Dingerkus & Uhler 1977, as modifed in Balon & Noakes 1980). A few adults were also cleared and stained for comparison, and to facilitate identification of skeletal structures. Thin sheets of dermal bone (e.g. operculum) were often only lightly stained, even in adults, and thus may have been present and calcified earlier than indicated. Cartilage bone undergoing dechondrification (see Cunningham 1982, Paine & Balon 1984) but not yet calcified is indicated as cartilage in the figures.

Age is given as days: hours: minutes after activation and represents the midpoint of the sampling interval. Periods, phases, and steps of ontogeny are named following Balon (1975b, 1980). Terminology for blood vessels and skeletal structures follows procedures and sources given in Paine & Balon (1984). Synonyms for many skeletal structures are given in the text to aid interpretation.

3. Results

3.1 Embryonic period (00:00:00–12:04:40)

3.1.1 Cleavage phase (00:00:00–01:06:10) – activation to organogenesis

Cleavage phase steps for rainbow darter were almost identical to those for logperch (Paine & Balon 1984); therefore only important differences are emphasized (see Fig. 1 for a comparison of the two species). Group 1 cleavage eggs ($n = 16$) were ovoid, 2.19 ± 0.06 mm along the long axis and 1.91 ± 0.05 mm along the short axis. The ovoid yolk and cytoplasm (i.e. including blastodisc) was 1.66 ± 0.06 mm by 1.56 ± 0.05 mm.

Step $C^1 1$ (00:00:00–00:01:40), Fig. 2. This step included activation, adhesion, cortical reaction, perivitelline space formation, bipolar differentiation, and fertilization, and ended with the appearance of the first cleavage furrow. Before activation, egg envelopes were closely applied to the yolk (Fig. 2a), but perivitelline space formation was com-

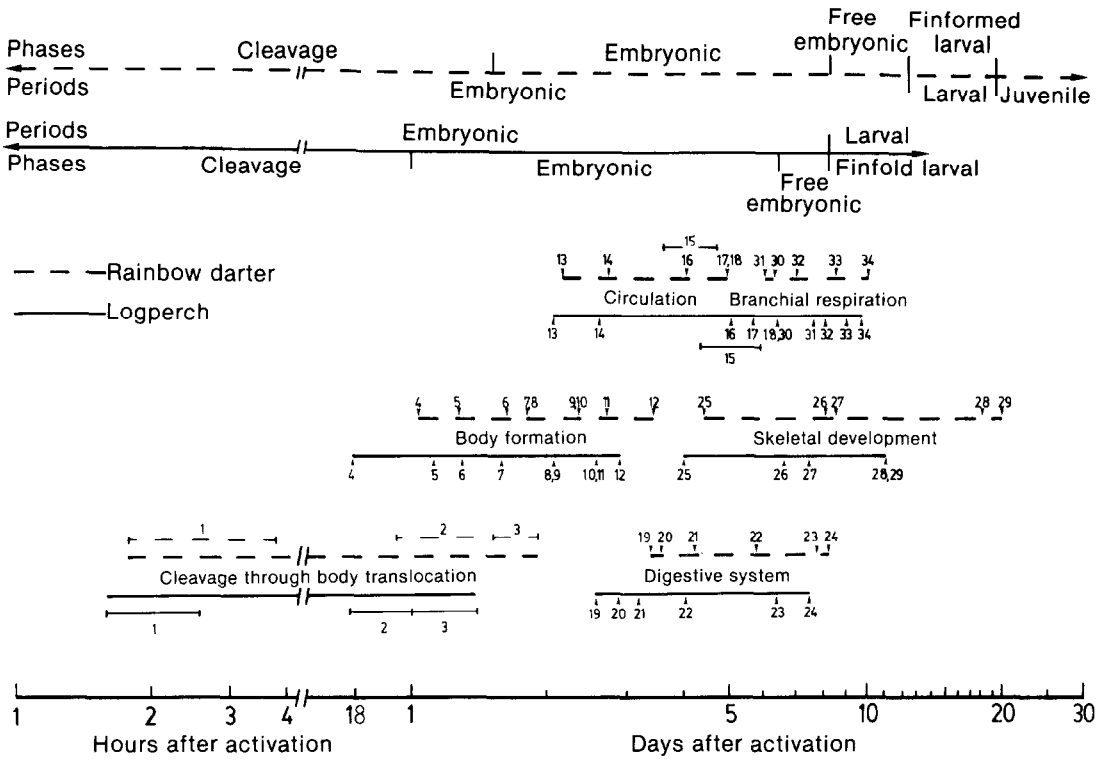

Ontogenic events

Cleavage through body translocation

1. cleavages 1 to 3
2. epiboly – germ ring visible to germ ring closure
3. body translocation – germ ring closure to head overlying oil globule

Body formation

4. neural plate
5. optic cups
6. Kupffer's vesicle
7. lenses
8. yolk melanophores
9. body contractions
10. body melanophores
11. final somite number attained
12. pectoral fin bud

Circulation

13. cardiac pulse
14. blood elements moving
15. dorsal segmental vessel formation
16. reversal of flow in posterior cardinal vein
17. caudal snare
18. hepatic artery, hepatic vitelline vein

Digestive system

19. liver
20. rectum
21. urinary bladder
22. pronephros
23. peristalsis
24. intestinal lumen

Skeletal development

25. cartilage (alcian blue stained)
26. jaw teeth
27. branchial basket complete except pharyngobranchials, basihyal
28. calcification (alizarin red S staining) of dermal bone
29. calcification of cartilage bone

Branchial respiration

30. flow through branchial arteries
31. mouth open
32. opercular aperture open
33. gill filaments
34. filamental arteries

Fig. 1. Comparison of timing and sequence of logperch and rainbow darter development.

pleted within 30 minutes. Each egg contained one large oil globule (0.7–0.8 mm in diameter) and several smaller ones. A thin blastodisc was evident 9 min after activation (Fig. 2b); by the end of this step it was 0.2 mm high (Fig. 2c). The micropyle was not nearly as obvious as it was in logperch eggs.

Step C²2 (00:01:40–00:20:50), Fig. 3. This step began with the first cleavage, and ended with the appearance of the germ ring and embryonic shield. The first cleavage occured roughly 10 min later than in logperch, and the second and third were further delayed (Fig. 1). The first three cleavages were horizontal, following the same pattern as in logperch (Fig. 3a–c). Subsequent vertical and horizontal cleavages produced first an irregular morula (Fig. 3d), then a rounded morula (Fig. 3e), which flattened during the remainder of the step (Fig. 3f).

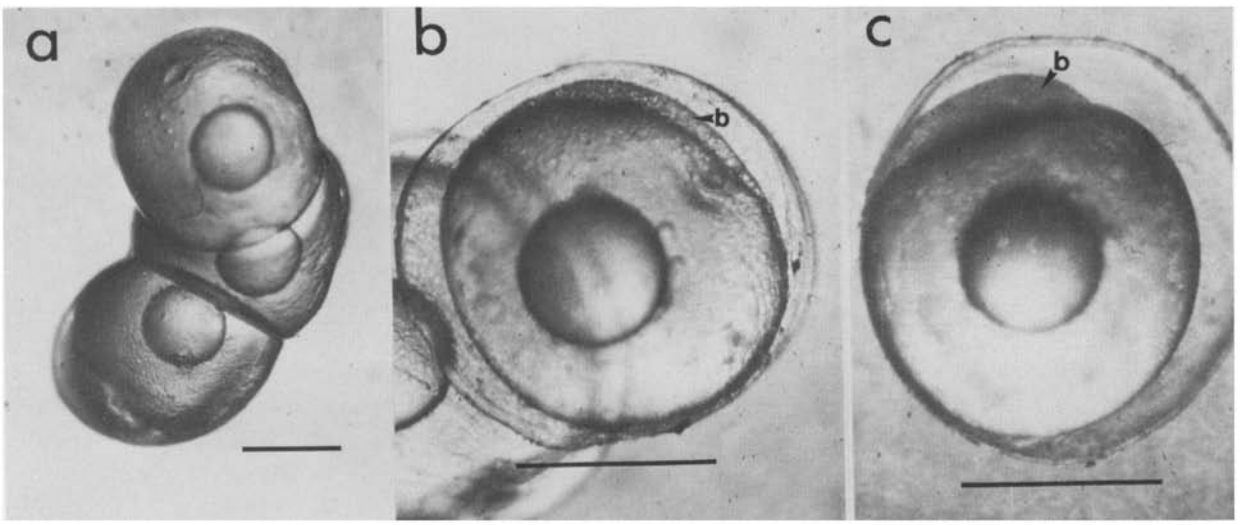

Fig. 2. Perivitelline space and blastodisc formation, vertical views from above, step $C^{1}1$: a – before activation; b – 9 min after activation; c – 90 min (b = blastodisc). Scales = 1 mm.

Step $C^{3}3$ (00:20:50–01:06:10), Fig. 4a–d. This step began with formation of the germ ring and embryonic shield, and finished with germ ring closure after epiboly. Epiboly was delayed relative to logperch, and perhaps as a result, some organogenesis occurred by germ ring closure (Fig. 1). The movement of cells over the oil globule took as long as movement over the yolk, as it does in walleye, *Stizostedion vitreum* (McElman & Balon 1979), and logperch. The neural plate was evident by 01:01:00 (Fig. 4c), and by germ ring closure optic vesicles, the notochord, and 3 somites were visible (Fig. 4d).

3.1.2 Embryonic phase (01:06:10–08:13:40) – organogenesis to active branchial respiration and hatching

Step $E^{1}4$ (01:06:10–02:04:05), Fig. 4d–f. This step began with germ ring closure, and ended with onset of cardiac pulse. At germ ring closure, the tail overlay the oil globule (Fig. 4d), but the body shifted relative to the oil globule until the head overlay the oil globule (Fig. 4f). By 01:21:25, the tail was free of the yolk. Somite number increased to 22, primarily during the first 12 h of the step. Optic vesicles formed optic cups by 01:10:35; lenses

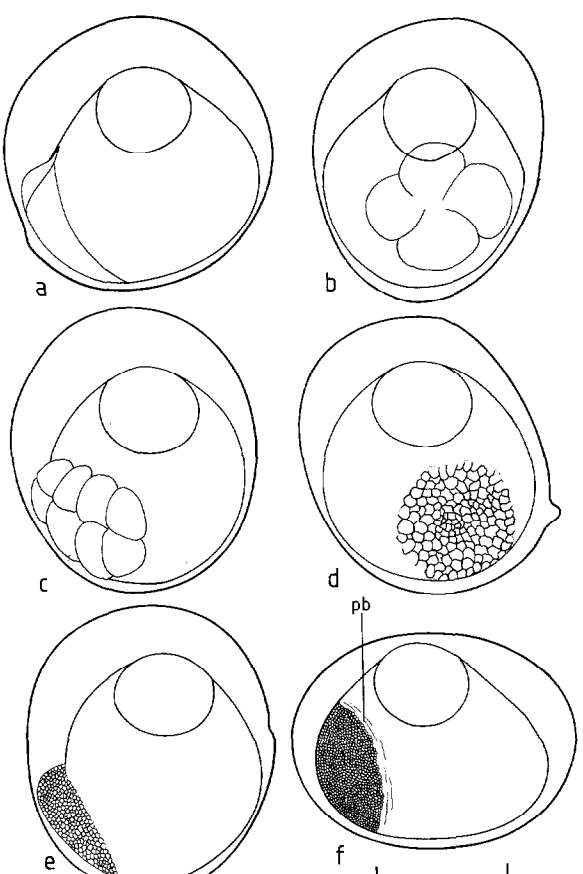

Fig. 3. Cleavage, horizontal views, step $C^{2}2$: a – first cleavage, 00:02:40; b – second cleavage, 00:02:50; c – third cleavage, 00:03:45; d – high morula, 00:06:25; e – high morula, 00:08:45; f – flat morula, 00:15:45; (pb = periblast). Scale = 1 mm.

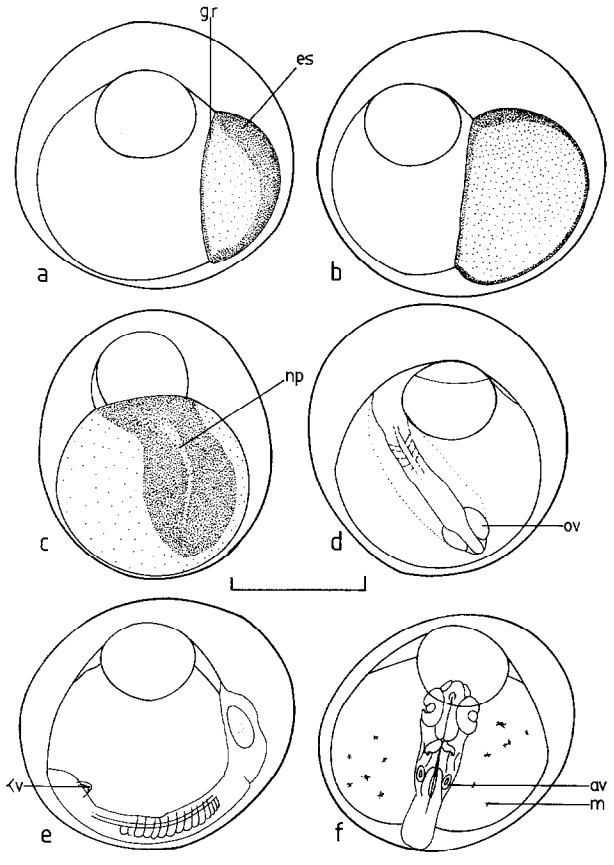

Fig. 4. Epiboly and organogenesis, steps $C^3$3 (a–c) and $E^1$4 (d–f): a – germ ring and embryonic shield, horizontal view, 00:21:00; b – 50% epiboly, horizontal view, 00:23:25; c – neural plate formation, horizontal view, 01:01:40; d – dorsal view, 01:06:25; e – left lateral view, 01:15:30; f – dorsal view, 02:00:45 (av = auditory vesicle, es = embryonic shield, gr = germ ring, Kv = Kupffer's vesicle, m = melanophore, np = neural plate). Scale = 1 mm.

were formed by 01:18:35. Auditory vesicles were evident by 01:12:40, olfactory vesicles by 01:15:10. The hindbrain was separated from the fore- and midbrain by a constriction at 01:15:10, and the cerebellum was visible 3 h later. The hindbrain was divided into neuromeres anteriorly by 01:21:35. Kupffer's vesicle(s) (paired in Fig. 4e, but unpaired in all subsequent specimens) was visible by 01:15:25. Yolk melanophores were evident by 01:18:35, earlier than in logperch.

Step $E^2$5 (02:04:05–02:17:15), Fig. 5a. This step began with the onset of cardiac pulse and finished when blood elements began circulating. Somite number increased to 36, and body movements were initiated. Heart beat rate was at first irregular, about 55 per min, but became regular, at 70 per min, by the end of the step. By 02:08:35, blood islands were visible on the yolk (Fig. 5a), and below the notochord preanally in the presumptive dorsal aorta.

Contraction of body muscles was first observed by 02:08:35. Movements cosisted of weak lateral body flexions, vertical head flexions, and very weak whole body contractions. Lateral flexions of the tail were common by the end of the step as the postanal trunk-tail was free of the yolk. Hatching gland cells appeared in the pericardial region by 02:08:35. Vesicles were present in what was presumably the liver region at the start of the step. The number and size of the yolk melanophores increased, and several melanophores were visible dorsally and postanally, and on the two anteriormost somites, by 02:08:35.

Step $E^3$6 (02:17:15 –03:13:20), Fig. 5b, c. This step began with the onset of blood circulation and ended with a sharp increase in heart beat rate, from 90–100 to 140 per min, concurrent with establishment of strong flow in the vitelline plexus. A largely unbranched vitelline network, along with some major body vessels, was laid down.

At the start of the step, blood elements flowed from the dorsal aorta to a single channel of the subintestinal vitelline vein on the left side of the yolk. Left and right channels were evident by 02:21:35 (Fig. 5b), joining on the left side just before emptying into the common cardinal veins at their juncture with the sinus venosus. The common cardinals were paired, formed on either side by the anterior and posterior cardinal veins. The posterior cardinal vein was unpaired posteriorly, where it branched from the newly visible caudal vein. Anteriorly it formed left and right branches, although in some subsequent specimens the left branch was not seen. The caudal vein was supplied by the caudal artery, a postanal extension of the dorsal aorta. Most of the flow from the caudal vein entered the subintestinal vitelline vein. Further anterior branching of the subintestinal vitelline vein was observed in subsequent specimens, but most of the

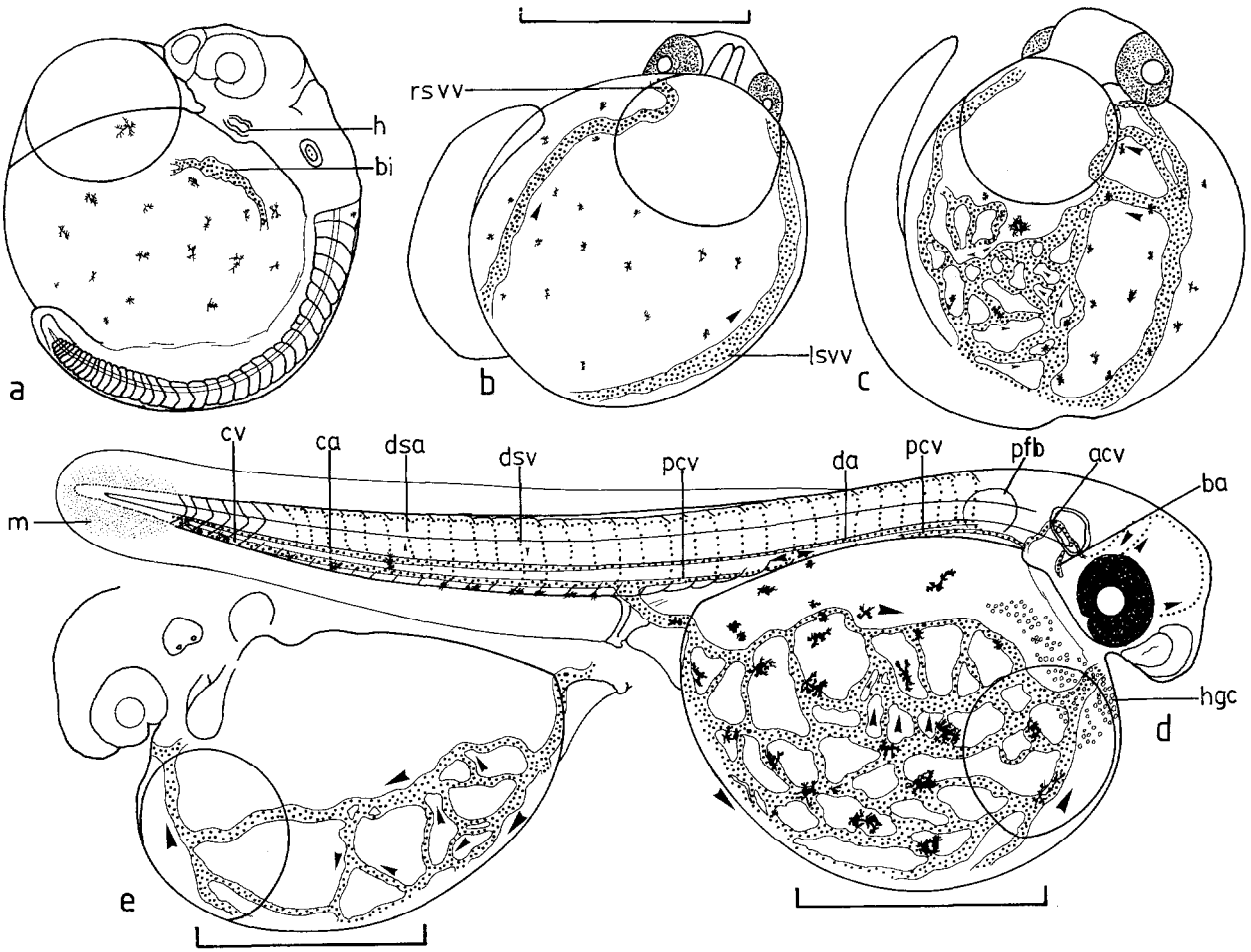

Fig. 5. Development of the circulatory system, excised embryos, steps E[35] (a), E[36] (b, c), E[47] (c–e): a – left lateral view, 02:08:35; b – ventral view, 02:21:35; c – ventral view, 03:13:20; d – right lateral view, 04:02:05; e – left lateral view of d (acv = anterior cardinal vein, ba = branchial artery, bi = blood island, ca = caudal artery, cv = caudal vein, da = dorsal aorta, dsa = dorsal segmental artery, dsv = dorsal segmental vein, h = heart, hgc = hatching gland cells, lsvv = left branch of subintestinal vitelline vein, m = mesenchyme concentration, pcv = posterior cardinal vein, pfb = pectoral fin bud, rsvv = right branch of subintestinal vitelline vein). Scales = 1 mm.

flow was carried in distinct left and right channels. Blood islands were visible on the yolk, and these were incorporated into the vitelline plexus in the next step. By 03:02:35, paired anterior aortae ran ventrally, anterior to the eye, turned dorsally, becoming the anterior cardinal veins, flowed dorsal to the eye and auditory vesicle, then ventrally and slightly posteriorly to form the common cardinal veins with the branches of the posterior cardinal vein. Vessels ran dorsally, from the aortae, to the anterior cardinal veins, across the eye. By 03:05:00 a vessel supplied the cranial region, and several smaller vessels appeared in the eye region.

The pectoral fin bud, 0.1 mm from base to tip, was visible by 03:09:05. The number of hatching gland cells increased in the area around the heart, and over the oil globule. The eyes were peppered with pigment by 03:01:15, and became darker by the end of the step. Melanophores increased in number on the yolk, in close association with the presumptive blood vessels, and appeared ventrally along the postanal trunk.

Step E⁴7 (03:13:20–04:05:50), Fig. 5c–e. This step began with a sharp increase in heart beat rate and ended with the establishment of the basic embryonic circulatory network. Cardiac pulse was 165 per min by the end of the step.

At the start of the step, blood was flowing through a number of anastomosing channels on the right side of the yolk, but through only one channel on the left side (Fig. 5c). In subsequent specimens, the left side usually had more branches (but see Fig. 5d,e). By the end of the step, the vitelline plexus reached its maximum extent, with a similar number of branches on each side.

Dorsal segmental vessels were present in the rectal region at the start of the step, and by the end, were present in all but the last 7 myomeres. By 04:02:05, flow had reversed in the posterior cardinal vein for 7 myomeres anterior to the rectum (Fig. 5d). Additional vessels appeared in the head, especially dorsally, during this step, with the anterior cardinal vein occupying a more ventral position relative to the auditory vesicle. The caudal artery extended to within 3 myomeres of the posteriormost by 03:21:40, and reached the last myomere by the end of the step. One branchial artery was visible by the end of the step.

A rectum was distinguishable at the start of the step, and by the end of the step the presumptive anus was swollen and protruded ventrally. The urinary bladder was also visible by the end of the step, although the pronephros was not observed until early in the next step. The somites were distinctly striated by 03:21:40, becoming myomeres. The specimen examined at the end of the step had 17 preanal and 22 postanal myomeres, but most of the specimens in this and subsequent steps had 15–16 preanal and 20 postanal myomeres. Mesenchyme was concentrated in the caudal finfold by the end of the step.

Step E⁵8 (04:05:50 – 06:06:55), Fig. 6a, 7a – e. This step began with the completion of the vitelline network, followed quickly by the appearance of the branchial arteries and the onset of chondrification. The step ended with establishment of passive branchial respiration. Heart beat rate remained steady at 160 per min; total length (TL) increased from 4.8 to 5.8 mm.

By 04:13:40, 3 branchial arteries were visible, and 5 h later 5 were visible. Blood first flowed through the arteries (= passive branchial respiration) by 05:08:05, although this was rarely the case for subsequent specimens. At this time, it was evident that the pseudobranchial artery was supplied by the combined hyoid and mandibular arteries. The specimen observed at 05:19:15 had lost the connection between the heart and the aortae, and instead all blood passed through the branchial arches. Loss of the embryonic branchial bypass was not observed again until the end of the step. By 06:02:20, the mouth was open, increasing the contact between the arches and the external medium.

The coeliacomesenteric artery supplied blood from the dorsal aorta to the hepatic artery by 04:23:05. No supraintestinal artery was observed during this step. Occasionally the subintestinal vein was observed, emptying into the liver, indicating that the supraintestinal artery was probably present. Blood from the liver capillaries was collected in the hepatic vitelline vein, which flowed across the left side of the yolk to join the left common cardinal vein.

By 04:13:35, the rectal dorsal segmental veins branched prior to entering the posterior cardinal vein or caudal vein (Fig. 6a). Throughout the step, the number of segmental veins that branched increased anteriorly and posteriorly. By 04:23:05, a caudal snare was formed, as the caudal artery crossed ventrally over the caudal vein near the last myomere, reversing the positions of the two vessels (Fig. 6a). By the end of the step the caudal artery extended almost to the tip of the notochord.

Over the course of this and the next few steps, the head lost its ventral flexure, assuming a more horizontal position (compare Fig. 5d with 6b). The auditory vesicle apparently ceased its anterior movement, as the distance from the posterior margin of the eye to the posterior margin of the vesicle increased from 0.2 to 0.4 mm. The pectoral fin grew from 0.2 to 0.3 mm from base to tip. The digestive tube was undifferentiated and usually only visible posteriorly. By the end of the step the liver was no longer smooth, but granular, in appearance. Ridges appeared on the anal protrusion.

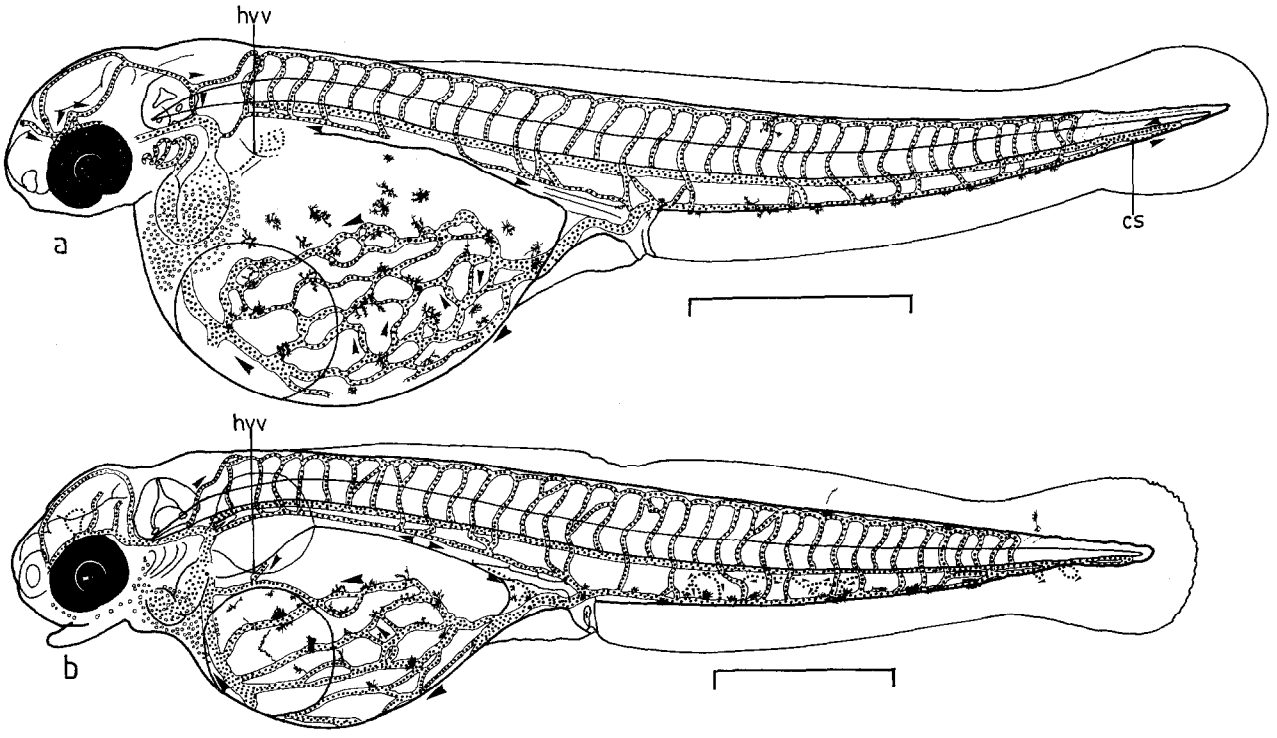

Fig. 6. Embryos excised from egg envelopes, left lateral views, steps E^{58} (a) and E^{69} (b): a = 05:11:55, b – 07:08:00 (cs = caudal snare, hvv = hepatic vitelline vein). Scales = 1 mm.

Hatching gland cells were observed dorsally on the head by 05:19:15.

The first alcian blue stained elements, the trabeculae and posterior margin of the eye ring, appeared by 04:08:30 (Fig. 7a). By 04:18:50, Meckel's cartilage was present but the eye ring was unstained (Fig. 7b, c). By 05:18:15, the eye ring was complete, the trabeculae were fused with the polar cartilages and parachordals, and the coracoscapula was visible (Fig. 7d, e). Small fused metaterygoid/quadrates and symplectic/hyomandibulars had also formed. Four small ceratobranchials and a ceratohyal were present on each side, along with the unpaired anterior copule (2nd and 3nd basibranchials ?). The posterior basicapsular commissure extended a small distance distally around the auditory vesicle, which contained a medial and ventral ribbon of cartilage. By 05:11:55, the ceratobranchials and ceratohyals had elongated, and the anterior basicapsular commissure extended slightly dorsally. One hypohyal was present, almost medially. The trabeculae were fused anteriorly to form an ethmoidal plate. By the end of the step, the hypohyal, hypobranchials, posteriormost epibranchials, pharyngeal cartilage (= 5th ceratobranchial or infrapharyngeal), and unstained maxillary were present on each side. In the pectoral girdle, the actinosal plate and unstained cleithrum were visible.

Melanophores appeared on the postanal midline by 04:08:30, and the postanal dorsum by 05:11:55. Melanophores external to the auditory vesicle, and one on the tip of the snout, were observed by 06:02:20. Yellow pigment, presumably carotenoids, appeared dorsally by 05:08:55, and was generally concentrated along blood vessels, particularly the dorsal longitudinal trunk. The pigment increased by the end of the step, especially around the cranial region.

Step E^{69} (06:06:55 – 08:13:40), Fig. 6b, 7f, g, 8a. This step began with the establishment of passive

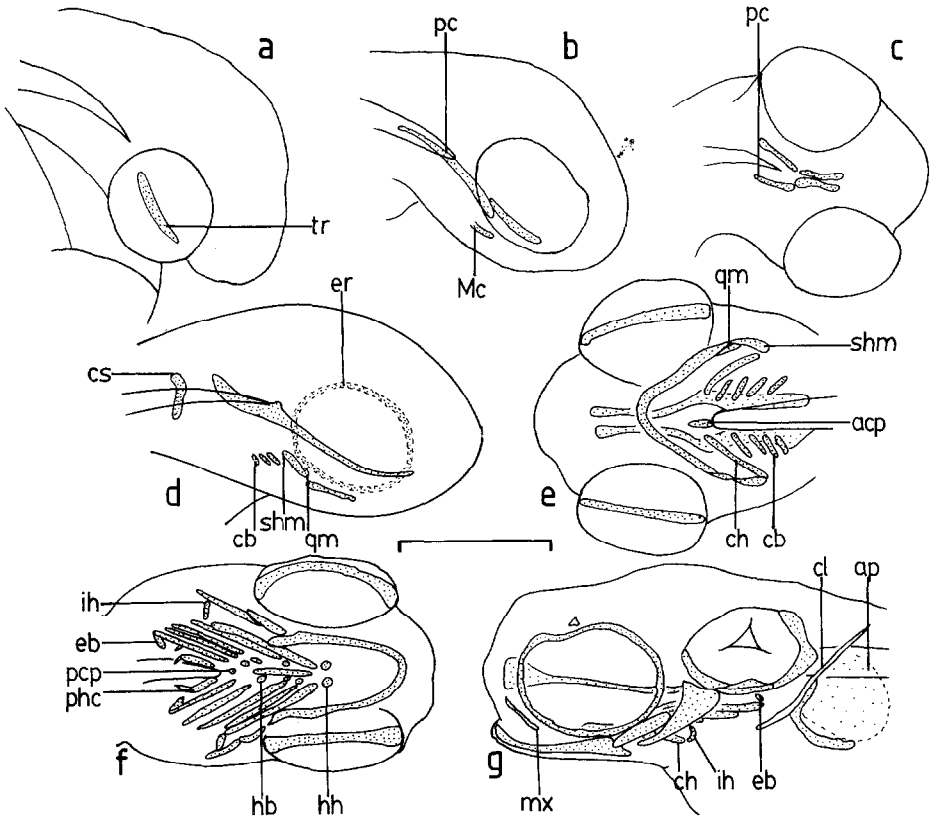

Fig. 7. Skeletal development in the head, alcian blue stained elements dotted, steps E^{5}8 (a–e) and E^{6}9 (f, g): a – right lateral view, 04:08:30; b – right lateral view, 04:18:50; c – dorsal view of b; d – right lateral view, 05:11:55, e – ventral view of d; f – ventral view, 07:08:00; g – left lateral view of f (acp = anterior copule, ap = actinosal plate, cb = ceratobranchial, ch = ceratohyal, cl = cleithrum, cs = coracoscapula, eb = epibranchial, er = eye ring, hb = hypobranchial, hh = hypohyal, ih = interhyal, Mc = Meckel's cartilage, mx = maxillary, pc = parachordal, pcp = posterior copule, phc = pharyngeal cartilage, qm = quadrate/metapterygoid, shm = symplectic/hyomandibular, tr = trabecula). Scale = 0.5 mm.

branchial respiration, with the branchial basket mostly completed, and ended part way through the hatching process, with the onset of active branchial respiration. During this step, the yolk elongated, the vitelline plexus diminished, the intestinal circulatory network expanded, and cutaneous circulation was established. Some differentiation of the digestive tube occurred. Heart beat rate increased to 180–190 per min, and TL to 6.7 mm.

Flow through the branchial arches was established at the start of the step. The hypobranchial artery, turning posteriorly and ventrally to supply the heart, was visible by 06:14:00, but its source among the arches could not be traced. By 07:02:15, filaments were present on the gill arches, and 'gulping' movements of the mouth were common. By the end of the step, the opercular aperture was open, allowing intake of water into the buccal cavity, past the gills, and out the aperture (= active branchial respiration).

As the branchial respiratory system was developing, the vitelline respiratory plexus declined. The number of vessels on the yolk diminished as the yolk elongated, so that there were only 3 or 4 main channels of the subintestinal vitelline vein on each side by the end of the step (compare Fig. 6a with 6b). In many specimens, the hepatic vitelline vein joined the subintestinal vitelline vein considerably posterior to the sinus venosus (Fig. 6b). Some subintestinal vitelline vein flow was diverted to the

subintestinal vein, which ran anteriorly below the gut, turning dorsally just prior to emptying ventrally into the liver. The supraintestinal artery, supplied by the coeliacomesenteric artery, ran posteriorly above the gut, emptying into the subintestinal vein. Although present at the start of the step, the supraintestinal artery and subintestinal vein were not always visible in subsequent specimens. The posterior mesenteric artery, arising from the dorsal aorta in the rectal region, was observed only at 07:19:30. This vessel supplied both subintestinal and subintestinal vitelline veins.

At the start of the step, cutaneous vessels were present in the rectal region. Arteries arose from dorsal segmental arteries at the midline, ran towards the surface, often branching there, one branch flowing anteriorly, the other posteriorly, to join segmental veins ventral to the aorta or caudal artery. At the same time, some segmental arteries looped over the dorsal longitudinal trunk before joining it. By 07:02:15, many segmental veins branched before entering the caudal vein; those branches running horizontally appeared to be the precursors of the profundal caudal vein (Fig. 6b). Later in this step, many anterior segmental veins looped below the posterior cardinal vein before joining it. By 07:19:30, ventral cutaneous circulation was provided by arteries originating at or near the origin of the segmental arteries. These vessels ran ventrally and distally, towards the body surface, often branching, then usually entered the caudal vein. Sometimes, however, these vessels ran dorsally along the myosepta to join segmental veins dorsal to the aorta or caudal artery. Additional arteries from the aorta or caudal artery ran obliquely (dorsally, posteriorly) to enter segmental veins near the dorsum of the notochord. Some segmental arteries branched near the top of the notochord, providing a vessel running obliquely towards the dorsal longitudinal trunk or segmental veins.

During this step, precursors of the extensive caudal plexus were established. Early in the step, small loops appeared in the caudal vein (Fig. 6b), and several small vessels connected the caudal artery and vein in the vicinity of the last myomere. At 08:01:55, a small vessel from the caudal artery ran ventrally onto the caudal finfold, splitting into 2 branches returning to the caudal vein. In this, and later, specimens, this vessel always ran over the first prominent melanophore on the caudal finfold.

The subclavian artery, originating from the dorsal aorta, and running ventrally onto the pectoral fin, was first observed at 06:20:40. The artery ran dorsally and posteriorly around the base of the fin, forming the subclavian vein, which emptied ventrally into the common cardinal (Fig. 8a). Little change from this pattern was observed during the rest of the step. The chin was supplied by a vessel originating near the junction of the hyoid and mandibular arteries at 07:19:30 (shown for an older specimen in Fig. 8d).

During this step, the yolk elongated, increasing from 1.8 to 1.9 mm length, and decreasing from 1.2 to 0.8 mm maximum depth. The pectoral fin was 0.8 mm from base to tip at the end of the step, and mesenchyme concentrations were evident by 07:08:00. The head lost its ventral flexure entirely by the time hatching began. The gut became more distinct, with a lumen evident by 08:01:55. Peristalsis began at 07:19:30. Hatching gland cells appeared on the upper jaw and just posterior to the eye by 07:08:00. Melanophores were present dorsally on the head and anterior myomeres early in the step, and dorsally on the median finfold by 07:08:00.

Skeletal development during this step was largely devoted to completion of the branchiocranium and pharyngeal jaws, chondrification of the auditory capsule, and the start of axial skeleton formation. By 08:01:55, 3 epibranchials were formed on each side, and by 08:13:40, all 4 pairs had formed. Two teeth were present on each pharyngeal cartilage by 06:14:00, and there were 3 by the end of the step. The unstained premaxillary was visible by 06:14:00, and the unstained dentary, with one tooth, by 08:01:55. At 08:13:40, two teeth were present on each dentary. A faint palatine, not joined to the metapterygoid/quadrate, was visible by the end of the step. By 06:14:00, there was cartilage around the posterior margin, and by 07:08:00 the anterior margin, of the auditory vesicle. The basicapsular commissures completely surrounded the vesicle ventrolaterally except for a

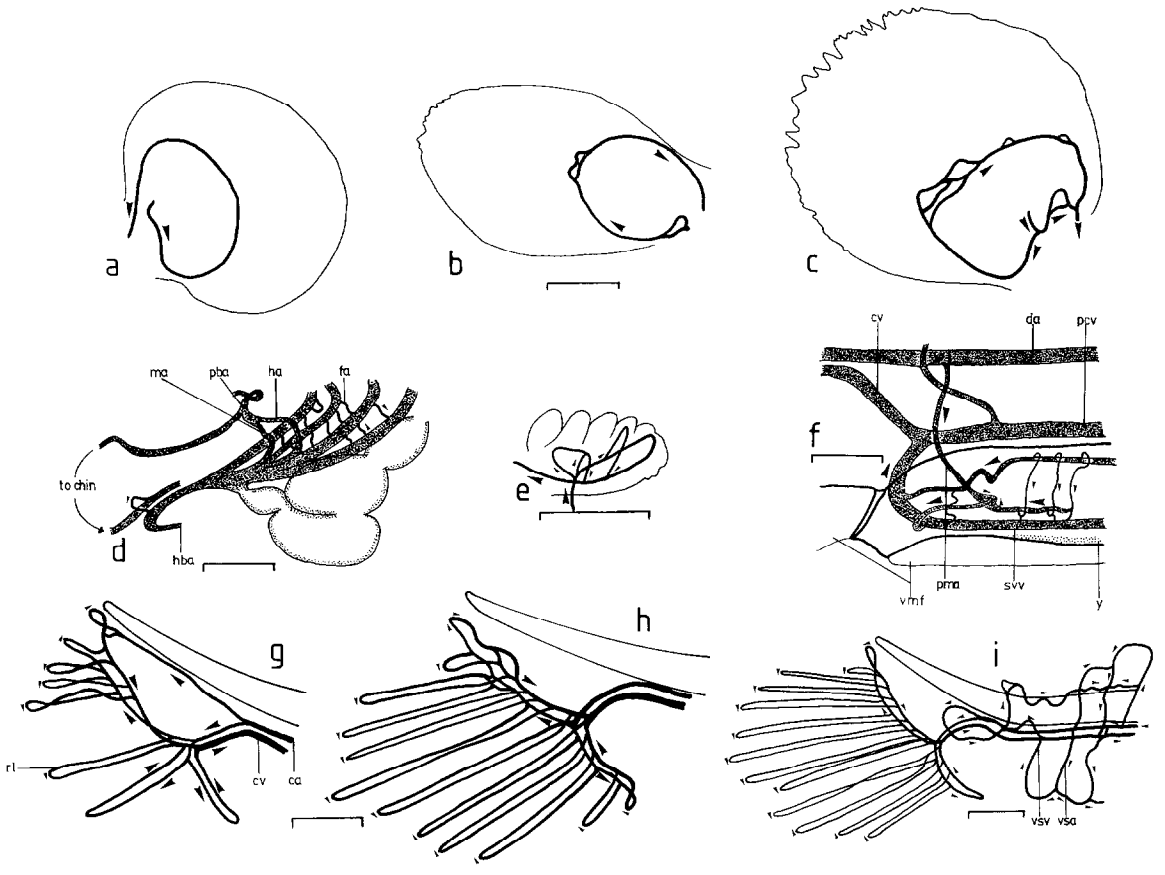

Fig. 8. Details of embryonic and larval circulation, steps E^{69} (a), $F^{1}10$ (b–e), $FF^{1}11$ (f–i): a – left pectoral fin, 07:08:00; b – right pectoral fin, 09:07:20; c – 11:00:30; d – heart and branchial arches, left dorsolateral view, 10:01:35; e – left pseudobranch, 12:00:30; f – rectal region, right lateral view, 16:03:35; g – caudal region, 13:18:15; h – 14:16:05, i – 15:15:35 (ca = caudal artery, cv = caudal vein, da = dorsal aorta, fa = filamental artery, ha = hyoid artery, hba = hypobranchial artery, ma = mandibular artery, pba = pseudobranchial artery, pcv = posterior cardinal vein; pma = posterior mesenteric artery, rl = radial loop, svv = subintestinal viteline vein, vmf = ventral median finfold, vsa = ventral segmental artery, vsv = ventral segmental vein, y = yolk). Scales = 0.2 mm.

small gap, by 07:08:00 (see Fig. 9a, an older specimen). At the same time, a small circle of cartilage formed above the eye which by the end of the step gave rise to a short, and medially incomplete, epiphyseal bar and the orbital commissures (= taenia marginalis). The anterior commissure was very short, but the posterior one extended almost to the anterior basicapsular commissure (Fig. 9a). Two hypurals formed by 08:01:55, and 4 by 08:13:40, along with 2 neural arches.

3.1.3 Free embryo phase (08:13:40 – 12:04:40) – active branchial respiration and hatching to onset of exogenous feeding

Step $F^{1}10$ (08:13:40 – 12:04:40), Fig. 8b–e, 9a–d, 10a,b. This step began with active branchial respiration, during the hatching interval, and finished with the onset of exogenous feeding and the beginning of median finfold differentiation. Other major events were continued absorption of the yolk and diminishment of the vitelline plexus, formation of the profundal caudal vein, formation of the axial skeleton, and increasing swimming activity. TL increased to 8.0 mm.

Duration and timing of the hatching interval varied among groups, but it generally occurred from 8 to 9 days after activation. Groups 3 and 4 were carefully observed during the entire hatching pro-

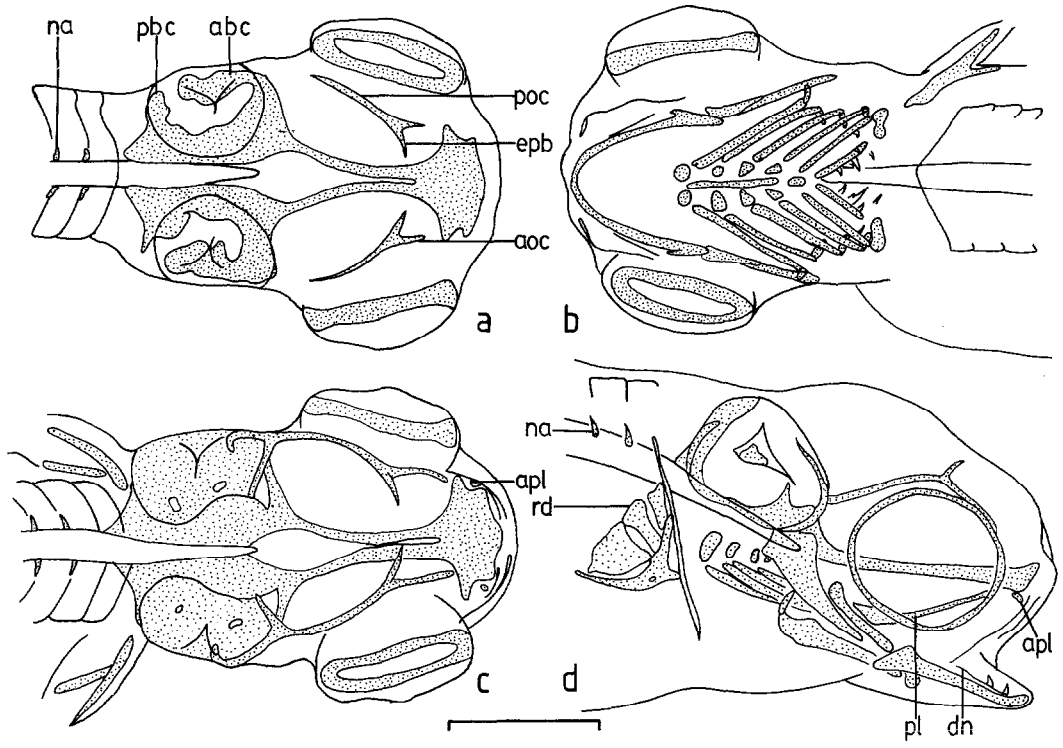

Fig. 9. Skeletal development in the head, alcian blue stained elements dotted, step F¹10: a – dorsal view, 08:18:00; b – ventral view of a; c – dorsal view, 10:01:35; d – right lateral view of c (abc = anterior basicapsular commissure; acc = anterior orbital commissure, apl = anterior tip of palatine, dn = dentary, epb = epiphyseal bar; na = neural arch, pbc = posterior basicapsular commissure, pl = palatine, poc = posterior orbital commissure; rd = radial). Scale = 0.5 mm.

cess; group 3 embryos hatched from 08:00:40 to 09:04:05, group 4 embryos from 07:23:00 to 08:17:35. The other groups were not closely monitored, but approximate median hatching time for group 2 was 09:04:00, and for group 5, 08:19:00. No phototropism, positive or negative, could be demonstrated after hatching, but free embryos remained benthic. By the end of the step, they were actively swimming, usually darting about on the bottom of the breeder boxes, but periodically venturing briefly into the water column.

During this step, the vitelline plexus diminished so that few branches of the subintestinal vitelline vein remained (Fig. 10a, b). The junction with the hepatic vitelline vein well posterior to the sinus venosus was not always present. By 09:19:25, flow had reversed in the posterior part of the subintestinal vitelline vein, where it previously branched from the caudal vein, so that it emptied into the posterior cardinal vein (Fig. 10a). At this time, the subintestinal vitelline vein was supplied by the posterior mesenteric and supraintestinal arteries. Various other patterns existed in subsequent specimens, but by the end of the step, and in later steps, the caudal vein did not supply the subintestinal vitelline vein.

As the vitelline plexus diminished, other potential respiratory networks expanded. Vigourous opercular movement was established by 09:07:20, and filamental arteries, connecting adjacent branchial arteries, were visible by 10:01:35 (Fig. 8d). By the end of the step, filamental vessels connected distinguishable efferent and afferent arteries within a single arch. The ventral caudal loop of the caudal artery expanded first posteriorly, then anteriorly (Fig. 10b), eventually providing the basis for the caudal plexus in subsequent steps. The subclavian artery produced a small plexus distally on the pec-

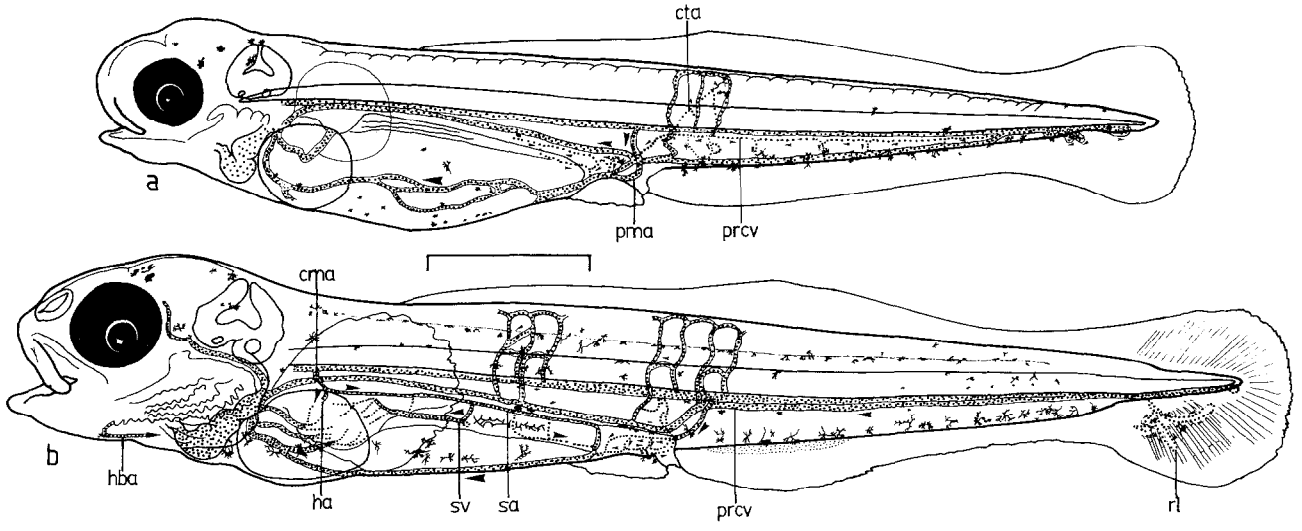

Fig. 10. Free embryo and larva, left lateral views, steps F[1]10 (a) and FFL[1]11 (b): a – 09:19:25; b – 12:04:40 (cma = coeliacomesenteric artery, cta = cutaneous artery, ha = hepatic artery, hba = hypobranchial artery, pma = posterior mesenteric artery, prcv = profundal caudal vein, sa = supraintestinal artery, sv = subintestinal vein). Scale = 1 mm.

toral fin (Fig. 8b, c). Both the caudal and pectoral plexuses may act as superficial respiratory networks, picking up oxygen from the surrounding water.

During this step, the profundal caudal vein replaced the inferior caudal vein (previously referred to as simply the caudal vein). At first the profundal caudal vein consisted of a series of small vessels, ventral to the caudal artery, running anteriorly or posteriorly (Fig. 10a). These vessels, originally emptying into the inferior caudal vein, were supplied by segmental veins, and posteriorly, by the inferior caudal as it crossed over the caudal artery. Gradually, more segmental veins flowed into the profundal caudal, and it aquired a consistent anterior flow, so that by the end of the step it was themajor vein posteriorly (Fig. 10b). The replacement of the inferior by the profundal caudal vein reduced the blood supply to the ventral part of the myomeres; this reduction was made up in later steps by the ventral segmental vessels.

By 09:02:35, it was possible to see that the pseudobranchial artery, formed from the hyoid and mandibular arteries, entered the pseudobranch, then exited to supply the eye (Fig. 8e). By 10:01:35, a small vessel connected the vein returning from the chin with the hypobranchial artery. The latter vessel should be derived from an efferent branchial artery, usually the fourth (Romer 1970), but this connection was never visible.

Skeletal development in the head during this step largely involved addition of teeth in the oromandibular and pharyngeal jaws, and expansion of the neurocranium and its connection via the palatine with the oromandibular jaws. By 08:18:00, the pharyngobranchials (= infrapharyngobranchials) were evident. By 12:00:30, there were 3 teeth on the medial edge, and one larger tooth posterior and distal to these, on each pharyngeal cartilage. There was one tooth on the left fourth ceratobranchial, and 3 teeth on each posterior pharyngobranchial. The basihyal (= glossohyal) was present as a small medial rod of cartilage anterior to the hypohyals. Two unstained branchiostegals were present on each side by 10:16:40, and 3 by 11:09:50. There were 3 teeth per dentary by 09:04:05, and 2 per premaxillary by 12:00:30. The anterior tips of the palatine were visible as separate cartilaginous structures at 10:01:35 (Fig. 9d), and fused with the posterior palatines by 10:08:55. At this time, the palatines had expanded at their junctions with the metapterygoid/quadrates.

By 09:04:05, the posterior orbital commissure extended to the auditory capsule; by 11:09:50, the

anterior commissure reached the anterior palatine. At the same time, the epiphyseal bar extended across the roof of the skull, connecting the orbital commissures from both sides. Therefore, during this step, the anterior skull roof became connected with both the auditory capsules and oromandibular jaws. The auditory capsules were completely surrounded basally by cartilage during this step, but there was no dorsal chondrocranium (Fig. 9a, c).

Throughout this step, 0 to 4 neural arches were present, except in two specimens. At 11:09:50, all neural arches were present, and at 12:00:30, the postanal hemal arches had formed as well. Obviously, vertebral arch formation occurs rapidly, as only a few anterior arches or the complete complement were visible in any one specimen. Five hypurals were present in the 2 specimens with all neural arches; the remaining specimens had 0 to 4. A few caudal rays were divided into 2 segments at 12:00:30; at the start of the next step there were some with 3 segments (Fig. 10b). First dorsal and anal pterygiophores (= radials) were also faintly stained blue at 11:09:50 and 12:00:30. By 10:01:35, the actinosal plate had split (Fig. 9d), beginning the process of radial formation. Four radials were visible by 10:08:55, and the bases for pectoral rays (= 2nd order radii or distal radials) were visible as small dots of cartilage by 11:09:50.

Peristalsis in the gut occurred throughout this step, and transverse ridges were evident by 09:12:50. The gall bladder and cystic duct were present by 10:01:35. One specimen at 10:16:40 had a small piece of prepared trout food in its gut, and a specimen at 10:18:50 had a ciliate in its gut. Because each of these fish had ingested only one item, it was probably accidental. Certainly, they were not feeding voraciously like the larvae in the next step.

3.2 Larval period (12:04:40 – 19:01:25)

3.2.1 Finformed larval phase (12:04:40 – 19:01:25) – beginning of exogenous feeding and differentiation of finfolds to complete differentiation of finfolds and formation of axial skeleton

Step FFL¹11 (12:04:40 – 19:01:25), Fig. 8f–i, 11, 12a, b. This step began with the onset of exogenous feeding and ended when the median finfolds had differentiated completely. Other major events were depletion of yolk, elimination of the subintestinal vitelline vein, expansion of the caudal plexus, formation of pelvic fins and a caudal fin with an axial lobe, completion of the chondrocranium, and appearance of gill rakers. TL increased to 9.6 mm. Head length (snout to posterior margin of auditory capsule) was >20% TL throughout this step, compared to 16–18% in the previous step.

Early in this step, the subintestinal vitelline vein had 1 to 3 branches per side and was connected anteriorly with the hepatic vitelline vein (Fig. 10b). Flow in the posterior part was often towards the posterior cardinal vein. At 16:03:35, the split between anterior and posterior flow of the now unbranched vein occurred at about the midpoint (Fig. 8f). In older specimens, only the anterior portion remained, and it eventually combined with the subintestinal vein, emptying into the hepatic capillaries. The number of vertically flowing vessels in the gut region increased substantially during this step (Fig. 8f).

The number of radial loops in the caudal plexus increased to 7 by 13:18:15 (Fig. 8g), and to 13 by the end of the step. At 13:18:15, the caudal artery extended to the notochord tip, but by 14:16:05, it extended only to the midpoint of the caudal plexus (Fig. 8g,h). A small posterior loop of the caudal artery was visible by 15:15:35 (Fig. 8i). At this time, ventral segmental arteries or veins were present in every postanal myomere except the last. Ventral segmental circulation had been present earlier, but consisted largely of remnants of the connections between dorsal segmental veins and the inferior caudal vein. The ventral segmental vessels later gave rise to circulation in the dorsal and anal fins. Horizontal segmental vessels appeared just dorsal to the notochord, and between the notochord and dorsal longitudinal trunk, by 17:16:10. Pectoral fin circulation changed during this step to a system resembling the caudal plexus. The subclavian artery ran around the distal edge of the muscle mass, producing loops running between rays. These loops drained into the subclavian artery, running proximal to the artery.

During this step, the yolk was entirely depleted. Most specimens were feeding voraciously on brine shrimp nauplii and cladocerans. Vigourous snapping motions of the jaws were common. By the end of the step, the larvae invariably swam into the water column and even to the surface as soon as food was introduced. When not feeding, they rested on the bottom. Little differentiation of the gut occurred, aside from an enlargement of the stomach region. Defecation was first observed at 17:02:05, and the gut contents were generally voided after that, whenever anaesthetic was applied. The liver expanded to the ventral body wall early in the step.

The anterior portion of the chondrocranium was completed in this step, by the addition of the paraphyseal bar and a medial connection between the epiphyseal bar and the dorsal roof of the cranium in the auditory capsule region (Fig. 11d). The medial connection, consisting of cartilaginous rods extending posteriorly from the epiphyseal bar and anteriorly from the dorsal cranial roof, was first observed by 13:18:35. The 2 rods were fused by 16:16:20. The epiphyseal bar had also expanded anteriorly by 18:03:10. The paraphyseal bar, formed by the fusion of the anterior orbital commissures dorsal to the ethmoidal plate, was visible by 13:18:35, and had expanded by 14:23:00. The anterior orbital commissures also expanded laterally by 17:16:10 (Fig. 11d). The exoccipital region of the otic cartilage expanded posteriorly, reaching the first neural arch by the end of the step (Fig. 11a, d). The shape of the chondrocranium changed during this step, as the anterior portion narrowed and

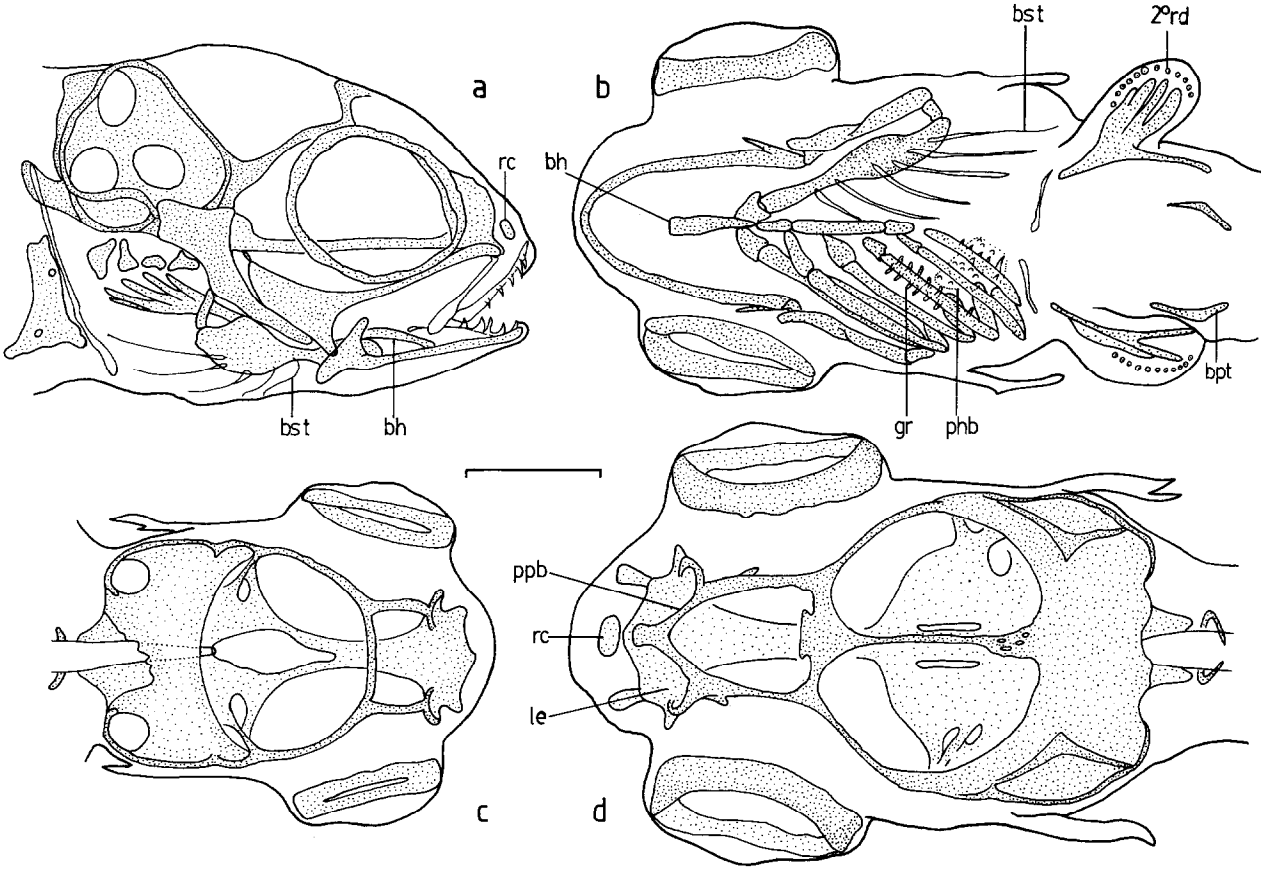

Fig. 11. Skeletal development in the head, alcian blue stained elements dotted, step FFL'11: a – right lateral view, 14:04:35; b – ventral view, 15:02:30; c – dorsal view, 12:12:15; d – dorsal view, 19:00:00 (bh = basihyal, bpt = basipterygium, bst = branchiostegal, gr = gill raker, le = lateral ethmoid, phb = pharyngobranchial, ppb = paraphyseal bar, rc = rostral cartilage, 2° rd = secondary radial). Scale = 0.5 mm.

lengthened relative to the whole (compare Fig. 11c with 11d). Because of the 2-dimensional nature of the views provided by the C&D microscope, this could represent straightening (relative to the rest of the head and body), as well as lengthening, of the anterior neurocranium.

Changes in the oromandibular jaws involved the formation of the rostral cartilage and expansion of the basiarticular process of Meckel's cartilage at 12:20:10, and continuous addition of premaxillary and dentary teeth (Fig. 11a). By 18:03:10, the premaxillary extended anterior and dorsal, and the maxillary ventral and posterior, to the rostral cartilage. Thus, the rostral cartilage could act as an axis for movement of these bones. At the same time, the dentary had expanded to invest the anterior Meckel's cartilage. Dentary, premaxillary, and maxillary were all calcified by this time, as indicated by their red colour after alizarin red S staining. At 13:01:25, a cartilaginous rod extended from the metapterygoid to the parachordals (Fig. 11a).

There were 4 branchiostegals by 12:20:10; the final complement of 6 (occasionally 7) per side was reached by 14:23:00 (Fig. 11b). Gill rakers appeared by 13:18:15 on all ceratobranchials. At this time the anterior and posterior copules were touching. The basihyal extended one third of the distance to the anterior margin of the jaw; by 15:02:30, it extended halfway. At that time, there were 5 teeth in the inner row on the pharyngeal cartilage, and one each in the medial and outer rows.

By 15:02:30, most of the neural and hemal arches were closed and spines were evident. The first neural arch was calcified by 18:03:10. At the start of the step, there were 6 anal, 11 first dorsal, and 9 second dorsal, proximal pterygiophores. The 7th anal proximal pterygiophore was visible at 13:01:25, the 8th at 15:02:30, and the 9th and last at 15:23:00. Two distal pterygiophores were present at 13:01:25, 4 by 14:04:35, 6 by 15:02:05, and 9 by 17:02:05. All 9 anal rays, including the double 9th, were present by 18:03:10 (Fig. 12a). There were two segments per ray, except the first 2. All dorsal proximal pterygiophores were visible by 17:16:10, all distal pterygiophores by 18:03:10. At this time, there were 10 unsegmented first dorsal rays (spines), and 13 second dorsal rays, including the last double ray. By 18:16:40, most second dorsal rays contained 3 segments. Usually 2 or 3 pterygiophores between the dorsal fins did not bear rays. As the median fins were forming, the finfolds were being resorbed. By 13:18:15, a cleft existed between the two dorsal fins; by 17:16:10, they were separated. At this time, the preanal finfold was not visible. All remnants of the embryonic median finfolds were gone by 19:01:25.

During this step, the formation of an asymmetrical caudal fin began (Fig. 12b). Rays formed first in the ventral part of the finfold; this part (hypochordal fin) could be distinguished from the dorsal part (axial lobe) containing mesenchyme. Not until the juvenile period, when all rays, including procurrent rays, had formed, did the caudal fin become externally symmetrical (Fig. 12c). At the start of the step, there were 5 hypurals and one epural. One hypural and one epural were added by 13:01:25. All hypurals bore rays by this time. The posteriormost epural was visible by 14:04:35. Both the posteriormost hypural and epural were reduced in size. By 15:02:30, there were 3 segments in most caudal rays; by 18:03:10, there were 4. The anterior 3 hypurals had fused basally, and there was a small ball of cartilage (remnant of a radial?) (Fig. 12b) between the last hemal spine and first hypural (actually the parhypural, but we retain the numbering scheme Schleuter & Thomerson (1971) use for the same species).

By 12:20:10, the pectoral fin rays took up alcian blue, and the 4 radials were joined only basally and distally. By 13:01:25, there were 11 rays; by 15:02:30, the final complement of 13 was attained. There were 4 segments in most rays by the end of the step. The cleithra expanded ventrally and medially, until they met at the ventral midline at 17:02:05. They were calcified by 18:03:10. A small rod of cartilage, the posterior part of the basipterygium, was visible on each side by 14:23:00, marking the beginning of pelvic girdle formation (Fig. 11b). The basipterygium expanded posteriorly by 17:02:05, and this expanded region bore 4 rays and one spine by 18:16:40.

Melanophores proliferated on the dorsum of the head, largely covering the cranial roof by the end of

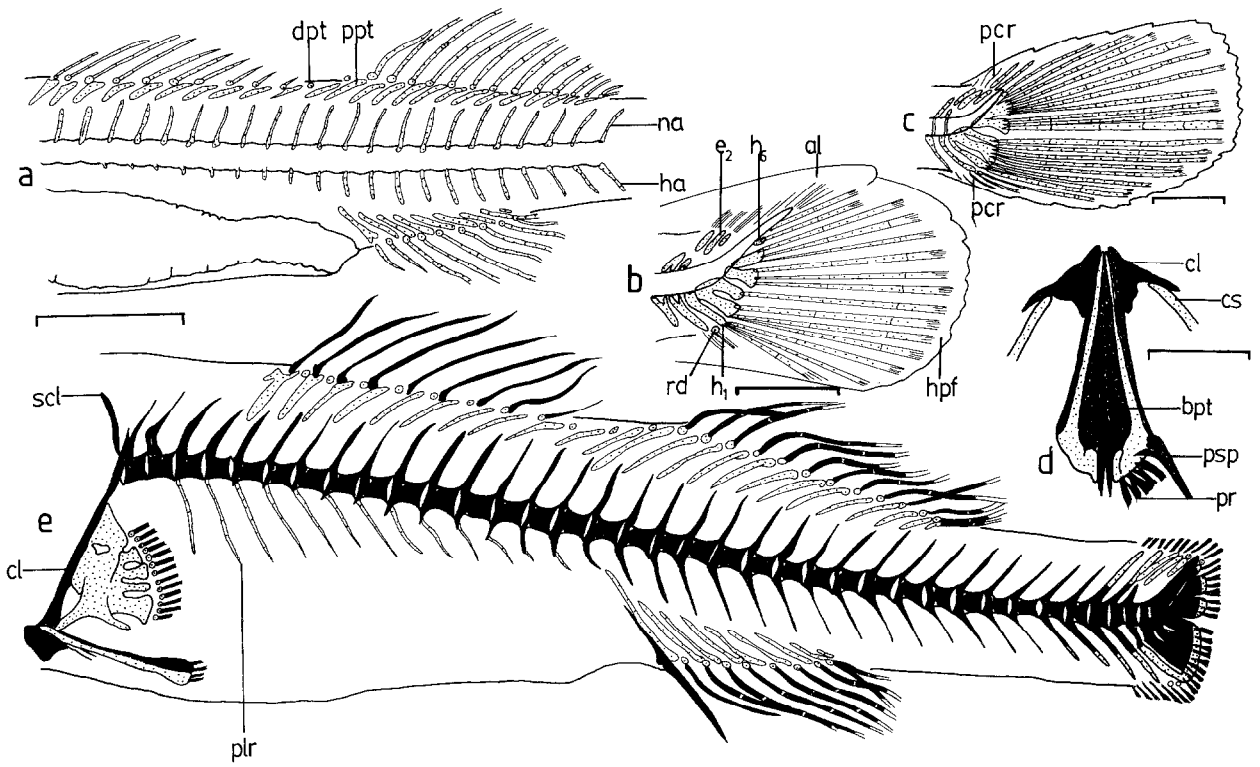

Fig. 12. Development of axial and appendicular skeletons, alcian blue stained elements dotted, alizarin red stained elements black, steps FFL^{1}11 (a, b), J^{1}12 (c), J^{2}13 (d, e): a – axial skeleton, 18:03:10; b – heterocercal caudal fin, 16:03:35, c – homocercal caudal fin, 28:04:00; d – pelvic girdle, ventral view, 43:03:00; e – axial skeleton, 43:03:00 (al = axial lobe, bpt = basipterygium, cl = cleithrum, cs = coracoscapula, dpt = distal pterygiophore, e_2 = second hypural, h_1,h_6 = first, sixth hypural, ha = hemal arch, hpf = hypochordal fin, na = neural arch, pcr = procurrent ray, plr = pleural rib, ppt = proximal pterygiophore, pr = pelvic ray, psp = pelvic spine, rd = radial (?), scl = supracleithrum). Scale for a, e = 1 mm; scales for b–d = 0.5 mm.

the step. Others formed on the snout, along the myomeres just dorsal to the gut, along the postanal myomeres just ventral to the notochord, on the body surface exterior to the notochord, and on the caudal fin.

3.3 Juvenile period (19:01:25 – ?)

Step J^{1}12 (19:01:25 – 29:16:30), Fig. 12c, 13. The transition from larva to juvenile really occurred from 18 to 21 d; 19:01:25 represents a rather arbitrary midpoint selected because the median ventral and dorsal finfolds were no longer evident at that time (Fig. 13). The last vestiges of the embryonic and larval periods, the oil globule and axial lobe, persisted until age 21 and 28 d respectively. The elimination of the axial lobe could arguably mark the completion of median finfold differentiation, the boundary of the juvenile period (Balon 1975b), making this the last larval step. The axial lobe was not always obvious later in the step, making this an equivocal characteristic to use in delineating periods. Instead, the formation of a jointed vertebral column, and separated, flexible median fins, both adult characteristics with important locomotory consequences, were used to mark the transition from larva to juvenile. Major events during this step were calcification of the axial skeleton, formation of the opercular bones, and articulation of the pelvic with the pectoral girdle. The step ended with the appearance of scales. Ages are given as days: hours; to claim any greater accuracy after 20 d would be unwise. The largest specimen (27:07) was 10.5 mm TL, 8.8 mm standard length (SL); the smallest (21:01) 9.6 mm TL, 7.7 mm SL.

The middle rays of the anal and second dorsal

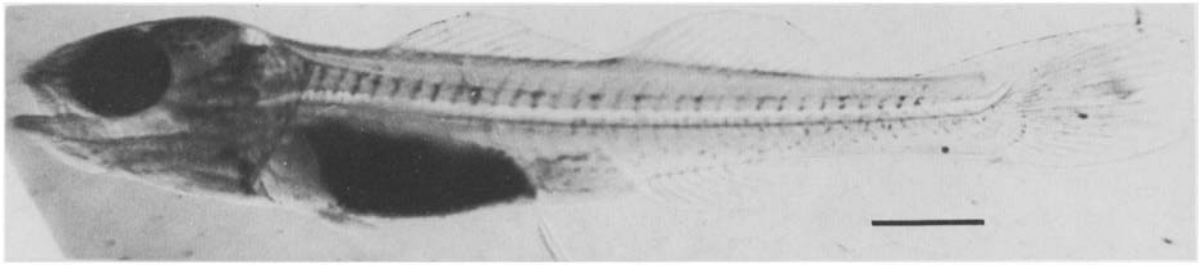

Fig. 13. Transition from larva to juvenile, left lateral view, 19:01:25. Scale = 1 mm.

fins were supplied by branches of the segmental vessels by 19:15. Circulation in the pelvic fins, derived from a branch of the subclavian artery, was established by the end of the step. Radial loops in the caudal fin extended almost to the tips of the rays. Two large vessels, one dorsal to the notochord, the other ventral to the dorsal aorta and caudal artery, were visible by 24:01. Flow was sluggish, in an anterior direction, in both vessels. A network of cutaneous vessels had formed on the dorsal surface of the head by 27:06. Secondary lamellar vessels were present in the gills by 24:01. Few other circulatory changes could be observed, as the specimens became more opaque.

The oil globule was rapidly depleted once the yolk had been used up, and was no longer present after 21:01. As in the previous step the head was the deepest part of the body (16–17% TL). Head length was 22–24% TL, preanal length 50–52% TL. No obvious changes occurred in the digestive system.

Calcification occurred in the parasphenoid (19:15), exoccipitals, and anterior tip of the notochord (22:02). The lateral ethmoid expanded posteriorly, past the anterior margin of the eye ring. The calcified angular was visible by 27:07; by this time, the dentary had almost completely invested Meckel's cartilage ventrally. The calcified opercle, consisting of a thin spine expanding anteriorly, appeared posterior to the hyomandibular by 19:15. By 27:06, the thin anterior edges of the preopercle, opercle, and subopercle stained red. By 21:01, the hypohyals articulated directly with the ceratohyals, and the hypobranchials with the ceratobranchials.

The anterior neural arches and spines were calcified, except dorsally, by 19:15, and the notochord was divided into distinct, but uncalcified, vertebrae. The vertebral column was calcified by 21:01, but this was not always true for subsequent specimens. Three cartilaginous pleural ribs were visible in one specimen by 27:06, which did not have a calcified vertebral column.

The first dorsal spines were calcified, except at their tips, by 19:23. Again, this was not always the case for older specimens. There were 3 segments in the anal fin rays by 23:04, and the first, spine bearing, proximal pterygiophore (= interhemal) was thickened relative to the others. There were 6 segments in the midcaudal fin rays by 27:06. By 28:04, the formation of procurrent rays from the epural and posterior hemal spines completed the formation of the homocercal caudal fin (Fig. 12c). At this time, the first 3 hypurals were fused at their tips as well as basally.

By 19:23, the basipterygium extended to near the anterior edge of the coracoscapula. The basipterygia articulated with the cleithra by 27:06. Each basipterygium bore 5 rays with 2 segments each, and one spine, by 23:04. Rays in the pectoral fin had 5 segments by 19:23. Calcified posterior extensions of the cleithra were visible in the ventral midline by 19:23.

Step J²13 (29:16 – ?), Fig. 12d, e, 14, 15. This step began with scale formation, and included the appearance of colour, adult melanophore patterns, and considerable calcification in the head. Sampling (along with the last fish) was terminated 47 days after activation. The largest specimen (47:21) was 12.3 mm TL, 9.9. mm SL; the smallest (39:19) 8.0 mm TL, 6.6 mm SL. Generally, large speci-

mens were more calcified than smaller ones of the same age, but the difference was minimal. Group 2 juveniles were usually larger and further developed skeletally than group 4 juveniles of similar age.

Two rows of scales were visible on the caudal peduncle of group 4 juveniles by 29:16 (Fig. 14). Curiously, scales did not appear in group 2 juveniles until 31:22, even though this group was more advanced in other respects. There were 3 to 4 rows of scales along the midline postanally in group 4 specimens by 32:22, and scales covered the body except the head, belly and nape by 37:01. Squamation in group 2 lagged about 2 days behind group 4.

By 33:22, the melanophores had aggregated posteriorly into vertical bars similar to those found in adults. Blue colour appeared intersegmentally by 39:20, and red pigment appeared exterior to the gut at the same time. Red was also present on the dorsal fins (43:03) and snout (47:21).

The spleen was visible early in the step, and the stomach became a definite sac. The expansion of the stomach was coupled with a slight looping of the intestine. No pyloric caecae were seen.

The exoccipitals and basioccipital were completely calcified by 31:22 (Fig. 15d). The pro- and pterotics began to calcify at the same time, and by the end of the study were almost entirely calcified (Fig. 15b, c). The sphenotics (= autosphenotics), prevomer, and toothed vomer were also calcified by the end of the study (Fig. 15c). Dorsally, the epiotics and anterior portion of the supraoccipital stained red (Fig. 15b). There was very little calcification in the parietal region.

Calcification also proceeded in the oromandibular jaws, branchial basket, and operculum. By 31:22, the calcified dentary had invested all of Meckel's cartilage except for the basiarticular process (Fig. 15d). The quadrate was calcified at its juncture with this process. Calcified areas, probably the dermal pterygoid bones, appeared ventral to the palatine, and anterior to the metapterygoid/quadrate, by 33:22 (Fig. 15e). The dorsal portion of the hyomandibular began to calcify by 39:20, and most of the remainder was calcified by 43:03. No calcification in the symplectic was observed. The ceratohyals were calcified anteriorly by 31:22 (Fig. 15a), and posteriorly, along with the interhyals, by 47:21 (Fig. 15e). The middle portions of the ceratobranchials and pharyngeal cartilages (bones?) were calcified by 31:22 (Fig. 15a). By this time, the opercle extended to the cleithrum; a definite oper-

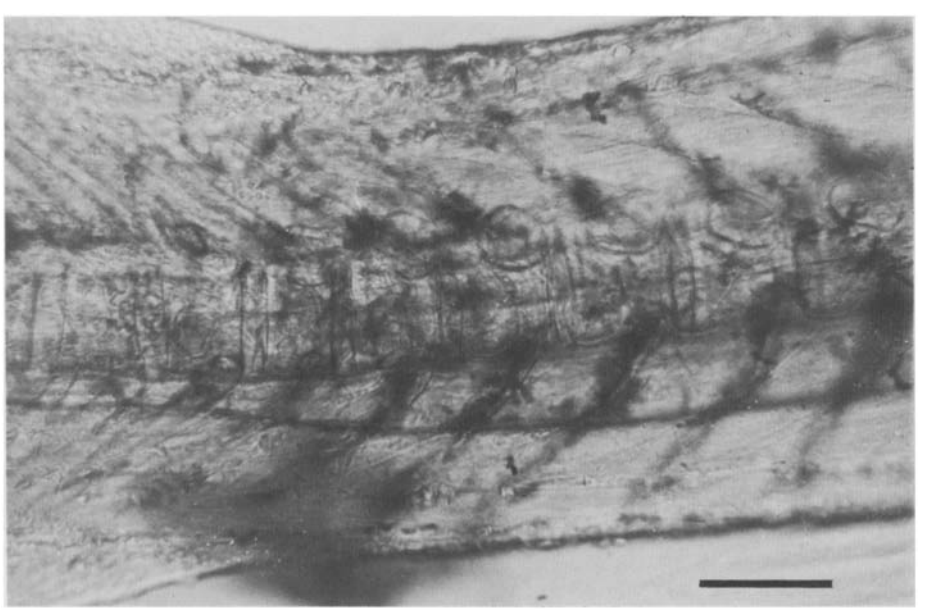

Fig. 14. Scale formation on the caudal peduncle, transition from step $J^{1}12$ to $J^{2}13$, 29:16:30. Scale = 0.2 mm.

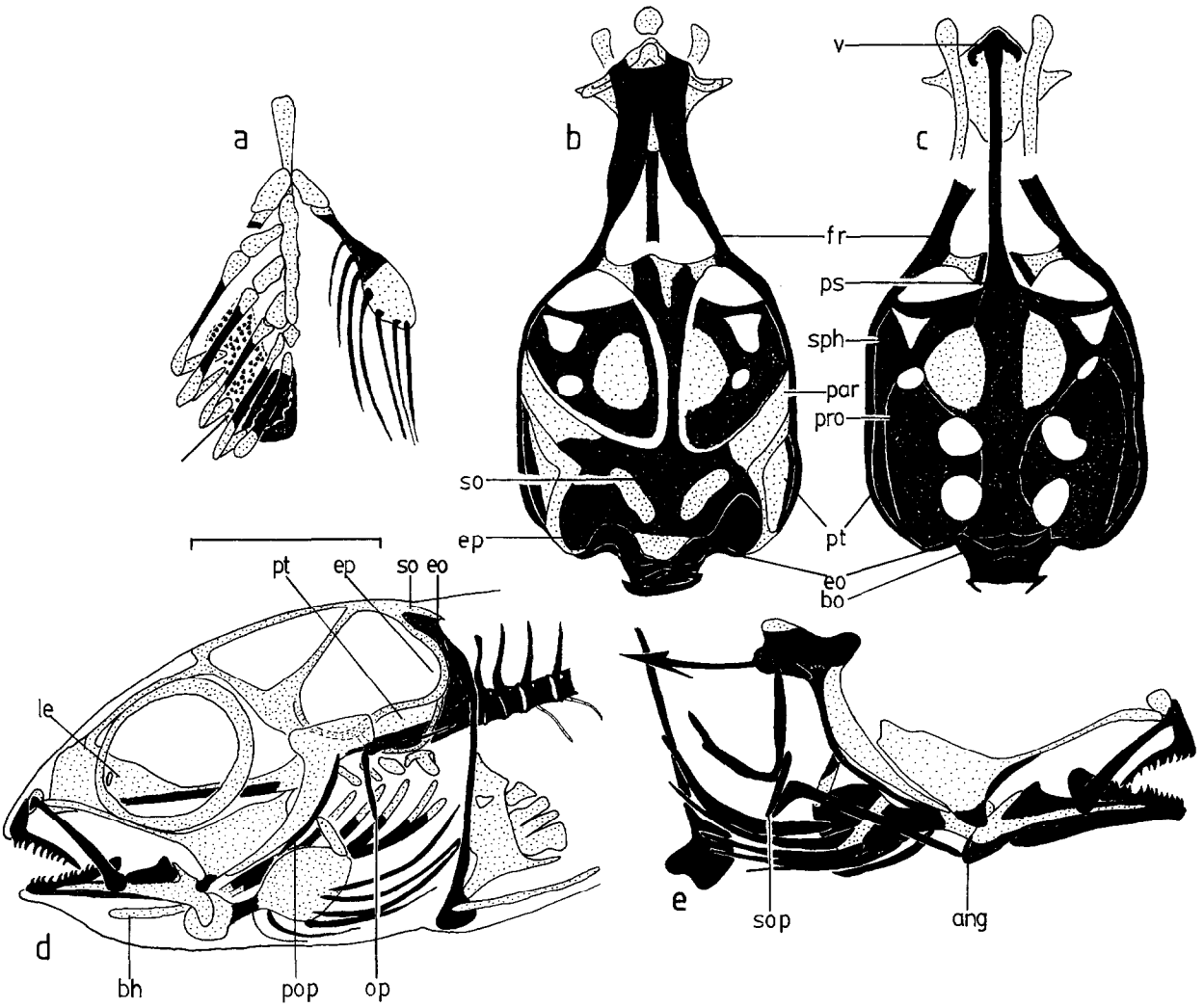

Fig. 15. Skeletal development in the head, alcian blue stained elements dotted, alizarin red S stained elements black, step J²13: a – branchial basket, ventral view, 31:22:00: b – neurocranium, dorsal view, 47:21:00: c – ventral view of b; d – left lateral view, 33:22:00; e – splanchnocranium, right lateral view, 47:21:00 (ang = angular, bh = basihyal, bo = basioccipital, co = exoccipital, cp = epiotic, fr = frontal, le = lateral ethmoid, par = parietal region, pop = preopercle, pro = prootic, ps = parasphenoid, pt = pterotic, op = opercle, so = supraoccipital, sop = subopercle, sph = sphenotic, v = vomer). Scale = 1 mm.

cular spine was visible by 43:03 (Fig. 15e). The ventroposterior edge of the opercle was evident by 47:21.

4. Discussion

In the following discussion, early development of the rainbow darter is correlated with environmental factors. The ontogenies of this and other percid species are compared, to show the ecological and evolutionary importance of differences in reproductive styles and early ontogenies. Evidence of the saltatory nature of ontogeny is presented throughout, but the main emphasis is on the role played by shifts in the timing of particular thresholds.

Steps of the cleavage and early embryonic phase for rainbow darter are similar to those for logperch (Paine & Balon 1984), except that germ ring clo-

sure and therefore body translocation are delayed (Fig. 1). Perhaps this reflects the fact that moving rainbow darter cells must cover a larger yolk. Formation of nervous system components and body segmentation does, however, precede muscular contraction in both species.

The development of logperch and rainbow darter begin to diverge more prominently after the onset of blood circulation; it appears that these later steps are of particular importance ecologically. Steps $E^{3}6$ to $E^{6}9$ are largely devoted to the development of respiratory structures. The vitelline plexus is expanded relative to that of the logperch, although both species deposit their eggs in gravel in lotic waters (Winn 1958a, b), and should therefore develop under similar oxygen regimes. The rainbow darter embryo is larger, with a lower surface area:volume, reducing the potential effectiveness of oxygen diffusion into the body, and may develop at higher temperatures and hence lower oxygen concentrations (Paine 1984). Accelerated development of the body circulatory system (Fig. 1) may occur for these reasons. Formation of the vitelline plexus occurs via a two part process. First, blood islands and two main branches of the subintestinal vitelline vein form (step $E^{3}6$), then flow in numerous capillaries formed from the blood islands commences, concommittant with a sharp increase in cardiac pulse (step $E^{4}7$). At the end of step $E^{4}7$, the vitelline plexus is of maximal size; subsequent diminishment with yolk depletion is compensated for by passive, then active, branchial respiration, and possibly, caudal and pectoral fin plexuses. As in logperch, chondrification of the branchial basket (step $E^{5}8$) precedes passive branchial respiration (step $E^{6}9$). Carotenoids appearing during step $E^{5}8$ may also serve a respiratory function (Balon 1977), but the evidence is still circumstantial (but see Karnaukhov 1979).

Hatching is coincident with active branchial respiration; perhaps ventilation is more efficient for a moving, as opposed to stationary, embryo. In addition, egg envelopes may simply be too restrictive for the elongating embryo. Because hatching is not associated with a change in behaviour (photoresponse) or environment, as it is in other percids (McElman & Balon 1979, Bulkowski & Meade 1983, Paine & Balon 1984), it is difficult to see why it should occur 4 days prior to exogenous feeding other than for respiratory reasons. Body elongation and expansion of the pectoral girdle in steps $E^{6}9$ and $F^{1}10$ may increase escape ability.

The onset of exogenous feeding is a decisive threshold, associated with a number of rapid morphological and behavioural changes. Rapid development of the axial skeleton, the beginning of ray formation in the median finfolds, increased head size, expansion of the palatines, and increased number of teeth in the jaws in the latter part of step $F^{1}10$ produce a strong, manoeuverable larva with well developed jaws. Increased swimming activity and vigourous snapping motions at the start of the larval period augment these morphological changes related to the switch to active predation. During the larval period, median and pelvic fins with segmented rays form, further enhancing swimming ability. The feeding apparatus is strengthened and altered as the dermal bones of the jaws expand, bear more teeth, and the anterior neurocranium elongates and narrows. A pointed snout, suitable for picking prey from crevices, is therefore formed. The expansion of the stomach region as the yolk diminishes increases the holding capacity of the digestive system.

The transition from larva to juvenile marks another important threshold. During this time the oil globule was depleted and calcification began. These two events combine to decrease buoyancy in the absence of swim bladder development, committing the juvenile to an obligatory benthic existence. The oil globule is also an endogenous food source; its depletion is presumably compensated for by expansion of the digestive system in the same space.

The second juvenile step began with the formation of scales, beginning posteriorly. The nape, breast, belly, and head are the last areas covered with scales in the walleye (Priegel 1964) and many darters (Braasch & Smith 1967, Page & Smith 1970, 1971, Page 1974, 1975, 1980, Page & Burr 1976, Burr & Page 1978, 1979, Cooper 1979, Page & Mayden 1981), and were not covered in this study. Reduced squammation in these areas, common in darters (Page 1983), may be associated with retardation of

scalation in conjunction with accelerated maturation. Squammation begins in the rainbow darter at a smaller size (10–12 mm TL) than in perch, *Perca flavescens* (21–22 mm TL, Norden 1961), or walleye (24 mm TL, Priegel 1964), but this represents a greater percentage of size at maturity or maximum size.

The second juvenile step is also marked by extensive calcification, particularily of the neurocranium. Further calcification and expansion of the frontals anterior to the supraoccipital, and of the parietals must still occur. At the end of the study, suborbitals, posttemporals, and postcleithra were still not visible. Calcification of the pectoral girdle had not begun, and the pterygiophores and pleural ribs were still cartilaginous. No epipleural ribs were visible.

Both squammation, and the remaining calcification, and even formation, of dermal bone that must occur have some bearing on the development of the lateralis system. Head canals in the adult are found in the suborbitals (infraorbital canal), frontal (supraorbital canal), calcified extensions running dorsally (supratemporal canal) and laterally (lateral canal) from the posttemporal, and the preopercle and dentary (preoperculomandibular canal). Some of these bones had not even formed by the end of the study; it is hardly suprising that few or no canal pores were observed in cleared and stained specimens. Pored scales of the lateral line form anteriorly first and therefore cannot form until the anteriormost scale in the lateral series has formed. We have already seen that development of squammation in the rainbow darter may be delayed (at least relative to maturation) compared to larger percids; perhaps this explains the incomplete lateral line in the rainbow and other darters. Retardation or truncation of canal formation may also be responsible for the reductions observed in the lateralis systems of darters, including the rainbow darter (Page 1977).

The essential differences between rainbow darter and logperch ontogenies can be seen as heterochronous shifts of important thresholds, consistent with the trend from small, pelagic, unprotected young with a prolonged larval period to large, demersal, protected young with a reduced larval period. The larger yolk of the rainbow darter embryo allows exogenous feeding to be delayed relative to the logperch (Fig. 1), producing a larger, better developed larva capable of feeding on aquatic insects directly. At the start of the larval period, rainbow darters are 2–3 mm longer than logperch, with heads about 50% larger. Drift to lentic areas (and planktonic food sources ?) is unnecessary, and the pelagic interval and finfold larval phase are eliminated. Rainbow darters can therefore remain in streams throughout their life cycle, and are, in fact, rarely found in rivers or lakes (Scott & Crossman 1973, Page 1983).

Rainbow darters are nonguarding, open substratum, rock and gravel spawners with benthic larvae (lithophils), one step removed from lithopelagophils such as logperch, walleye, and ancestral percids (Balon et al. 1977, Paine & Balon 1984) in the guild hierarchy (see Balon 1975a, 1981c for guild descriptions). The elimination of the pelagic interval appears to be a key adaptation, associated with the proliferation of *Etheostoma* species in streams (Paine 1984). Therefore, the major habitat shift in the North American darters, from rivers to streams, is coincident with a change in ontogeny resulting in a shift to a new guild.

Acknowledgements

The authors thank the Natural Sciences and Engineering Research Council of Canada for its support in the form of graduate scholarships to MDP and operating grant A9538 to EKB. Dwight Watson and Rick Procter provided help in the field; Cam Portt arranged for permission to sample from the Ontario Ministry of Natural Resources, Cambridge District.

References cited

Balon, E.K. 1975a. Reproductive guilds of fishes: a proposal and definition. J. Fish. Res. Board Can. 32: 821–864.

Balon, E.K. 1975b. Terminology of intervals in fish development. J. Fish. Res. Board Can. 32: 1663–1670.

Balon, E.K. 1977. Early ontogeny of *Labeotropheus* Ahl, 1927 (Mbuna, Cichlidae, Lake Malawi), with a discussion on advanced protective styles in fish reproduction and development. Env. Biol. Fish. 2: 147–176.

Balon, E.K. 1979. The theory of saltation and its application in the ontogeny of fishes: steps and thresholds. Env. Biol. Fish. 4: 97–101.

Balon, E.K. 1980. Chapters on the ontogeny of charrs. pp. 485–666, 703–720. *In*: E.K. Balon (ed.) Charrs: Salmonid Fishes of the Genus *Salvelinus*, Dr. W. Junk Publishers, The Hague.

Balon, E.K. 1981a. Saltatory processes and altricial to precocial forms in the ontogeny of fishes. Amer. Zool. 21: 573–596.

Balon, E.K. 1981b. About processes which cause the evolution of guilds and species. Env. Biol. Fish. 6: 129–138.

Balon, E.K. 1981c. Additions and amendments to the classification of reproductive styles in fishes. Env. Biol. Fish. 6: 377–389.

Balon, E.K. 1983. Epigenetic mechanisms: reflections on evolutionary processes. Can. J. Fish. Aquat. Sci. 40: 2045–2058.

Balon, E.K. 1984a. Reflections on some decisive events in the early life of fishes. Trans. Amer. Fish. Soc. 113: 178–185.

Balon, E.K. 1984b. Patterns in the evolution of reproductive styles in fishes. pp. 35–53. *In*: C.W. Potts & R.J. Wootton (ed.) Fish Reproduction: Strategy and Tactics, Academic Press, London.

Balon, E.K. & D.L.G. Noakes. 1980. Principles of ichthyology. 3rd revised edition. Department of Zoology, College of Biological Science, University of Guelph, Guelph. 285 pp.

Balon, E.K., W.T. Momot & H.A. Regier. 1977. Reproductive guilds of percids: results of the paleogeographical history and ecological succession. J. Fish. Res. Board Can. 34: 1910–1921.

Braasch, M.E. & P.W. Smith. 1967. The life history of the slough darter, *Etheostoma gracile* (Pisces, Percidae). Ill. Nat. Hist. Surv. Biol. Notes 58. 12 pp.

Bulkowski, K. & J.W. Meade. 1983. Changes in phototaxis during early development of walleye. Trans. Amer. Fish. Soc. 112: 445–447.

Burr, B.M. & L.M. Page. 1978. The life history of the cypress darter, *Etheostoma proeliare,* in Max Creek, Illinois. Ill. Nat. Hist. Surv. Biol. Notes 106. 15 pp.

Burr, B.M. & L.M. Page. 1979. The life history of the least darter, *Ehteostoma microperca,* in the Iroquois River, Illinois. Ill. Nat. Hist. Surv. Biol. Notes 112. 15 pp.

Cooper, J.E. 1979. Description of eggs and larvae of fantail (*Ehteostoma flabellare*) and rainbow (*E. caeruleum*) darters from Lake Erie tributaries. Trans. Amer. Fish. Soc. 108: 46–56.

Cunningham, J.E.R. 1982. Early ontogeny of *Adinia xenica* (Cyprinodontiformes, Fundulidae): some patterns and processes of epigenesis. M.Sc. thesis, University of Guelph, Guelph. 198 pp.

Dingerkus, G. & L.D. Uhler. 1977. Enzyme clearing of alcian blue stained whole small vertebrates for demonstration of cartilage. Stain Technol. 52: 229–232.

Ginsberg, A.S. 1963. Sperm-egg association and its relationship to the activation of the egg in salmonid fishes. J. Embryol. Exp. Morphol. 11: 13–33.

Karnaukhov, V.N. 1979. The role of filtrator molluscs rich in carotenoid in the self-cleaning of fresh waters. Symp. Biol. Hung. 19: 151–167.

McElman, J.F. & E.K. Balon. 1979. Early ontogeny of walleye, *Stizostedion vitreum,* with steps of saltatory development. Env. Biol. Fish. 4: 309–348.

Norden, C.R. 1961. The identification of larval yellow perch, *Perca flavescens* and walleye, *Stizostedion vitreum.* Copeia 1961: 282–288.

Page, L.M. 1974. The life history of the spottail darter, *Etheostoma squamiceps,* in Big Creek, Illinois, and Ferguson Creek, Kentucky. Ill. Nat. Hist. Surv. Biol. Notes 89. 20 pp.

Page, L.M. 1975. The life history of the stripetail darter, *Etheostoma kennicotti,* in Big Creek, Illinois. Ill. Nat. Hist. Surv. Biol. Notes 93. 15 pp.

Page, L.M. 1977. The lateralis system of darters (Etheostomatini). Copeia 1977: 472–475.

Page, L.M. 1980. The life histories of *Etheostoma olivaceum* and *Etheostoma striatulum,* two species of darters in central Tennessee. Ill. Nat. Hist. Surv. Biol. Notes 113. 14 pp.

Page, L.M. 1983. Handbook of darters. T.F.H. Publications, Neptune City. 271 pp.

Page, L.M. & B.M. Burr. 1976. The life history of the slabrock darter, *Etheostoma smithi,* in Ferguson Creek, Kentucky. Ill. Nat. Hist. Surv. Biol. Notes 99. 12 pp.

Page, L.M. & R.L. Mayden. 1981. The life history of the Tennessee snubnose darter, *Etheostoma simoterum* in Brush Creek, Tennessee. Ill. Nat. Hist. Surv. Biol. Notes 117. 11 pp.

Page, L.M. & P.W. Smith. 1970. The life history of the dusky darter, *Percina sciera,* in the Embarras River, Illinois. Ill. Nat. Hist. Surv. Biol. Notes 69. 15 pp.

Page, L.M. & P.W. Smith. 1971. The life history of the slenderhead darter, *Percina phoxocephala,* in the Embarras River, Illinois. Ill. Nat. Hist. Surv. Biol. Notes 74. 14 pp.

Paine, M.D. 1984. Ecological and evolutionary consequences of early ontogenies of darters (Etheostomatini). Env. Biol. Fish. 11: 97–106.

Paine, M.D. & E.K. Balon. 1984. Early development of the northern logperch, *Percina caprodes semifasciata,* according to the theory of saltatory ontogeny. Env. Biol. Fish. 11: 173–190.

Priegel, G.R. 1964. Early scale development in the walleye. Trans. Amer. Fish. Soc. 93: 199–200.

Romer, A.S. 1970. The vertebrate body. 4th edition. W.B. Saunders Co., Philadelphia. 601 pp.

Schlueter, R.A. & J.E. Thomerson. 1971. Variation in the caudal skeleton of *Etheostoma caeruleum* Storer. Copeia 1971: 332–334.

Scott, W.B. & E.J. Crossman. 1973. Freshwater fishes of Canada. Bull. Fish. Res. Board Can. 183. 966 pp.

Taylor, W.R. 1967. An enzyme method of clearing and staining small vertebrates. Proc. U.S. Nat. Mus. Washington 122: 1–17.

Winn, H.E. 1958a. Observations on the reproductive habits of darters (Pisces, Percidae). Amer. Midl. Nat. 59: 190–212.

Winn, H.E. 1958b. Comparative reproductive behavior and ecology of fourteen species of darters (Pisces, Percidae). Ecol. Monog. 28: 155–191.

Received 18.12.1983 Accepted 10.2.1984